Mechanical Systems and Signal Processing 46 (2014) 114–128

Contents lists available at ScienceDirect

Mechanical Systems and Signal Processing

journal homepage: www.elsevier.com/locate/ymssp

On the derivation of the pre-lockup feature based condition monitoring method for automatic transmission clutches

Agusmian Partogi Ompusunggu *

Flanders' Mechatronics Technology Centre (FMTC), Celestijnenlaan 300D, 3001 Heverlee, Belgium

ARTICLE INFO

Article history:
Received 5 May 2013
Received in revised form
24 November 2013
Accepted 27 December 2013
Available online 21 January 2014

Keywords:
Wet friction clutches
Automatic transmissions
Condition monitoring
Engagement duration
Slip distance

ABSTRACT

This paper discusses how a qualitative understanding on the physics of failure can lead to a theoretical derivation of effective features that are useful for condition monitoring of wet friction clutches. The physical relationships between the features and the mean coefficient of friction (COF) which can be seen as the representation of the degradation level of a wet friction clutch are theoretically derived. In order to assess the accuracy of the theoretical relationships, Pearson's correlation coefficient is applied to experimental data obtained from accelerated life tests on some commercial paper-based wet friction clutches using a fully instrumented SAE#2 setup. The analyses on the experimental data reveal that the theoretical predictions are plausible.

1. Introduction

Vehicles have become indispensable utilities in our modern society. Designs of vehicles have evolved from basic transportation utilities into advanced modern vehicles that can satisfy the increasing demands of the society for safety, driving comfort, high energy efficiency, low cost, high power capacity, *etc*. In a vehicle, a transmission system is one of the key devices that is responsible to accomplish the aforementioned requirements. A transmission system is defined as a device having the function to transfer power from the engine to the wheels, *via* the axles. The increasing sophistication of modern vehicles is also accompanied by the growing complexity of the transmission system.

In recent years, original equipment manufacturers (OEMs) have launched different types of transmission on the automotive market which can be, in general, classified into two main groups, namely (i) manual systems and (ii) semi or fully automatic system. A manual system consists of traditional Manual Transmission (MT), while the automatic system can be of different types, such as traditional Automatic Transmission (AT), Automated Manual Transmission (AMT), Continuously Variable Transmission (CVT), and Power Shift Transmission/Dual Clutch Transmission (DCT). As is obvious from its name, an automatic system is a transmission that shifts power or speed by itself, while the manual system involves the driver to do so.

Fig. 1 shows the annual sales ratios of manual and automatic systems with respect to the total annual sale of all transmissions from the years 2001 till 2015 [1,2]. The trends reveal that the drivers' perspective has changed since the last decade. It is also obvious from the figure that the global economic recession occurring in 2008 and 2009 impacted the customers' response on the selection of the transmission, which seemed to be only temporarily. Vehicles with manual

* Tel.: +32 16 32 80 42; fax: +32 16 32 80 64.
E-mail addresses: agusmian.ompusunggu@gmail.com, agusmian.ompusunggu@fmtc.be
URL: http://www.fmtc.be

0888-3270/$ - see front matter © 2014 Elsevier Ltd. All rights reserved.
http://dx.doi.org/10.1016/j.ymssp.2013.12.015

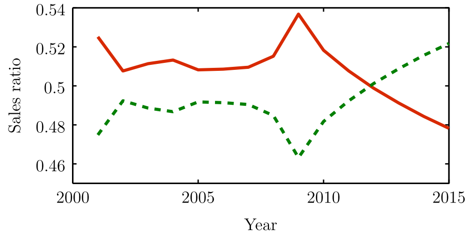

Fig. 1. Ratios of annual sales of manual systems (solid line) and automatic systems (dashed line) w.r.t the total annual sales of all kinds of transmissions on the global market.

systems have dominated the global automotive market for decades. However, the demand for the manual system is on the wane; and as predicted, the automatic systems will be dominating the global automotive market after the year 2012. This tendency is probably due to the fact that automatic systems offer more attractive capabilities that can satisfy the demands of our dynamic society, compared to the manual system [3].

Despite gaining popularity, there are some issues in automatic transmission systems that have been addressed and been attracting attention of many researchers across the world, namely energy efficiency improvement, emission reduction and driving performance enhancement. Modeling and simulation of the automatic systems have been carried out by many researchers in order to better understand the transmission behavior [4–7]. This understanding can serve as a basis for optimizing the transmission design and developing control strategies. Different advanced control strategies for automatic systems have been proposed in the literature, for example see Refs. [8–12], mostly focusing on improving fuel economy and enhancing gearshift quality.

Although considerable solutions related to the above-mentioned issues have been achieved, nevertheless, maintenance aspects were overlooked and they recently gain attention [13–16]. In fact, maintenance has also to be regarded as an important issue for the development of reliable automatic systems. An appropriate maintenance strategy on these transmissions is a necessity because of their vital function in the vehicles. While the complexity of automatic systems increases, the requirement for a maintenance strategy becomes more crucial. Undoubtedly, inevitable degradation occurring in the transmissions can change the vehicles′ performance. As the degradation progresses, failure can unexpectedly occur, which eventually leads to the total breakdown of the vehicles. Therefore, integration of a maintenance strategy into automatic transmission systems can significantly increase safety and availability/reliability and reduce the maintenance cost of the vehicles.

Condition Based Maintenance (CBM), which is also known as Predictive Maintenance (PdM), is a right-on-time maintenance strategy which is driven by the actual condition of the critical component(s) of any systems of interest. This concept requires technologies and experts, in which all relevant information, such as performance data, maintenance histories, operator logs and design data, are combined to make optimal maintenance decisions [17]. It has been realized that this maintenance strategy can significantly increase safety and availability/reliability and reduce the maintenance cost of systems of interest. PdM has been in use since 1980s and successfully implemented in various applications such as in oil platforms, manufacturing machines, wind turbines, automobiles, electronic systems [18–23].

In general, the key technologies for realizing the PdM strategy rely on three basic ingredients, namely (i) *condition monitoring*, (ii) *diagnostics* and (iii) *prognostics*. Condition monitoring (CM) aims at assessing the condition of a system/component of interest by means of tracking the change of a parameter that indicates a degradation progress. In the PdM research community, the parameter to be monitored is often referred to as a *relevant feature*. Diagnostics helps the maintenance engineer to localize and identify the fault type in a system/component. Finally, prognostics aims at predicting the remaining useful life (RUL) of a system/component at which the system/component will no longer perform its intended function. The RUL is estimated by means of forecasting the time interval needed by the feature to reach a pre-defined threshold that represents the end-of-useful life. Hence, (1) a *feature* to be monitored, (2) a *degradation model* which can be heuristically or physically derived, and (3) a *threshold* are critical aspects to succeed in development of the PdM strategy.

To realize the PdM strategy for automatic transmission systems, the critical component(s) therefore needs first to be identified. Afterwards, the condition monitoring, diagnostics and prognostics system for the critical component must be developed. For automatic transmission systems, wet friction clutches are one of the critical components. This consideration is based on the fact that the performance and long-term durability of such transmission systems are strongly determined by the clutch [24]. A brief introduction of wet friction clutches comprising the working principle and typical failure modes is discussed in Section 1.1.

1.1. *Wet friction clutches and the failure mechanisms*

Besides being used for automatic transmission systems, wet friction clutches are also widely used for limited slip differentials (LSDs) in all-wheel-drive (AWD) vehicles [25]. The LSD allows the AWD vehicles to have better maneuverability under severe road conditions. The forthcoming paragraphs only focus on the function, working principle of wet friction clutches that are widely employed in heavy duty transmissions such as ATs and DCTs.

1.1.1. Function and working principle

Wet friction clutches (or wet clutches) are mechanical components enabling the power transmission during the operation from the engine to the wheels, based on the friction occurring on lubricated contacting surfaces. The clutch is lubricated by an automatic transmission fluid (ATF) having a function as a cooling lubricant cleaning the contacting surfaces and giving smoother performance and longer life. However, the presence of the ATF in the clutch reduces the coefficient of friction (COF). In applications where high power is necessary, the clutch is therefore designed with multiple friction and separator discs. This configuration is known as a multi-disc wet friction clutch as can be seen in Fig. 2, in which the friction discs are mounted to the hub by splines, and the separator discs are mounted to the drum by lugs. In addition, the input shaft is commonly connected to the drum-side, while the output shaft is connected to the hub-side. The friction disc is made of a steel-core-disc with friction material bonded on both sides and the separator disc is made of plain steel.

As a mechatronic system, a wet friction clutch is typically integrated with an electro-mechanical-hydraulic actuator that is used for engaging/disengaging. This actuator consists of some main components, such as a piston and a returning spring, which is always under compression and a hydraulic group consisting of a control valve, an oil pump, *etc*. As can be seen in Fig. 2, the piston and the returning spring are assembled in the interior of a wet friction clutch. To engage the clutch, pressurized ATF that is controlled by the valve is applied through the actuation line in order to generate a force acting on the piston. When the applied pressure exceeds a certain value to overcome the resisting force arising from both spring force and friction force occurring between the piston and the interior part of the drum, the piston starts moving and eventually pushes both friction and separator discs toward each other. To disengage the clutch, the pressurized ATF is released such that the returning spring is allowed to push the piston back to its rest position.

In general, the complete duty cycle of a wet clutch can be classified into four consecutive phases: (i) *fully disengaged*, (ii) *filling*, (iii) *engagement* and (iv) *fully engaged* phase, as illustrated in Fig. 3. In the fully disengaged phase ($t < t_f$), *i.e.* prior to the clutch actuation, the returning spring holds the piston at its rest (re-tracked) position so the two elements, *i.e.* friction and separator discs, are to rotate independently with the rotational velocities of ω_i and ω_o, see the top leftmost scheme in

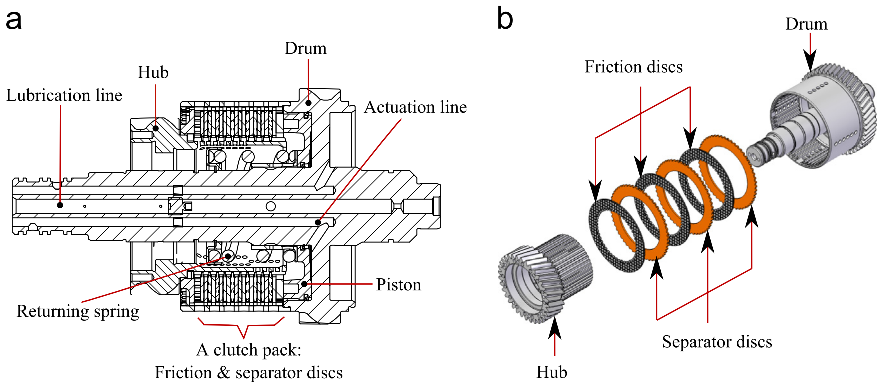

Fig. 2. The configuration of a multi-disc wet friction clutch, (a) cross-sectional and (b) exploded view.

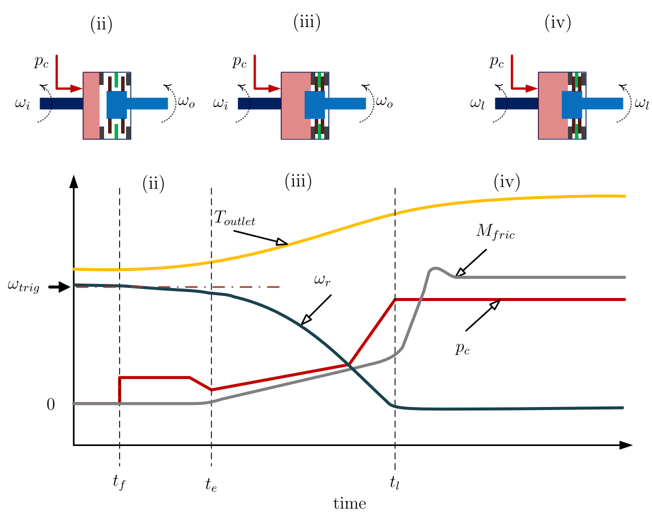

Fig. 3. A typical duty cycle of a wet friction clutch and the illustration of (ii) *filling*, (iii) *engagement* and (iv) *fully engaged* phase.

the figure. Meanwhile, a *controller routine* that needs to be embedded in the Engineering Control Unit (ECU) of a vehicle equipped with an automatic transmission checks the input rotational velocity ω_i and the output rotational velocity ω_i of the clutch. When the two rotational velocities are about certain values, say $\omega_i \approx \omega_{i,trig}$ and $\omega_o \approx \omega_{o,trig}$, a control signal is then sent to a hydraulic valve for the clutch actuation. Equivalently, the control signal is sent when the relative rotational velocity (sliding velocity) $\overrightarrow{\omega_r} = \overrightarrow{\omega_i} - \overrightarrow{\omega_o}$, with $\overrightarrow{\bullet}$ denoting vector operation, is about a certain value, say $\omega_r \approx \omega_{trig}$. It is important to note here that such a routine is necessarily implemented in the ECU in order to realize an accurate clutch condition monitoring system as will be theoretically discussed in Section 3. The latter phase is called the filling phase which occurs between time instant t_f and t_e. During the engagement phase ($t_e < t < t_l$), the clutch is actuated by gradually increasing the ATF pressure such that gentle contacts between the friction and the separator discs can be established. As a result, the transmitted friction torque increases gradually with the increasing ATF pressure. Because of the increasing friction torque, the relative rotational velocity gradually decreases until it reaches zero value ($\omega_r \to 0$), meaning that the discs are now to rotate with about the same rotational velocities of ω_l as illustrated in the top rightmost scheme of the figure. As sliding (rubbing) in the engagement phase constitutes an irreversible process, some portion of the transmitted energy is converted into heat which consequently results in an increase of the ATF temperature. The time instant when the sliding velocity reaches zero value for the first time is called the *lockup time* t_l. After this time instant, the clutch enters the fully engaged phase ($t > t_l$) wherein the relative rotational velocity remains around zero value. From now on, the event before the lockup time instant t_l is referred to as the *pre-lockup phase* while otherwise is referred to as the *post-lockup phase*.

1.1.2. Failure modes in wet friction clutches

Despite great achievements in the performance and durability, the friction material and ATF of wet friction clutches still suffer from inevitable aging processes (degradation) while the transmissions are under operation. Failures of the friction material and ATF are the two major failure modes occurring in a wet friction clutch. These two failure modes can occur as a consequence of different mechanisms, as schematically depicted in Fig. 4. The figure shows that the degradation mechanisms of both failure modes are very complex and inter-related with each other. Mechanical (adhesive) wear and thermal degradation (carbonization) are the main degradation mechanisms of friction material failure. While, the ATF failure results from several mechanisms, namely oxidation, thermal decomposition, evaporation, tribochemical wear and hydrolysis. These mechanisms are briefly discussed in the following paragraphs.

Degradation mechanisms of the friction material: Surface damage is the major degradation mechanisms occurring in the clutch friction material. This is mainly caused by the sludge/deposition of the ATF degradation products and/or of debris particles from the friction material and possibly from other components, *e.g.* separator material. The deposition gradually transfers and penetrates into the worn friction material surface while it is under sliding, finally clogging the pores of the friction material surface [26–28]. This surface transformation is known as the *glazing* phenomenon where the friction material loses its surface porosity and appears smooth and shiny. However, this terminology is not universally defined within the community. Newcomb et al. [29] promoted the use of the term "glazed" to describe damage of friction materials resulting *only* from the deposition of fluid degradation products on the friction material surface. When the pore blockage (*i.e.* by the deposition) takes place, the ability of the friction material to squeeze out the fluid during the engagement process deteriorates. This deterioration is revealed by the increase of the permeation time of ATF on the friction material surface as the glazing level proceeds, as reported by Maeda and Murakami [30]. Consequently, an oil film is easily formed on the glazed surface, thus reducing asperity-to-asperity contacts, which eventually leads to the decrease of the kinetic COF.

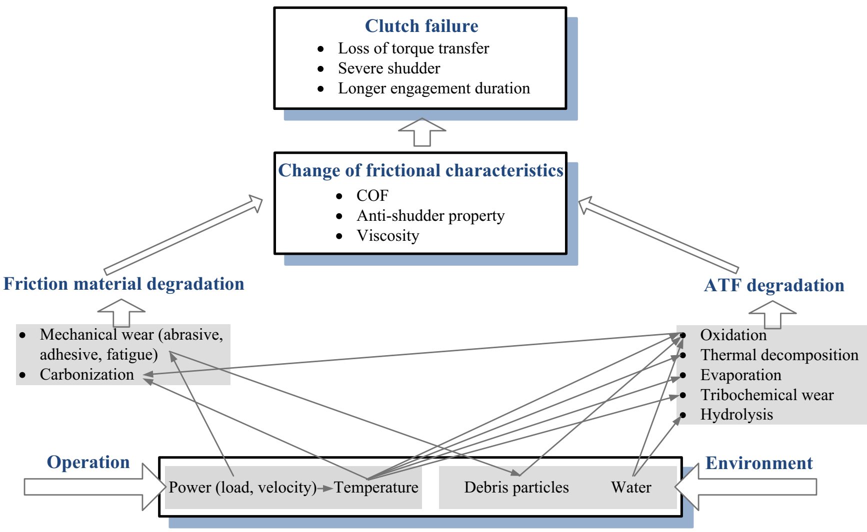

Fig. 4. Inter-relation among the clutch degradation mechanisms.

Degradation mechanisms of ATF: As shown in Fig. 4, the degradation occurring in an ATF can be caused by many possible mechanisms. Oxidation is the most predominant reaction experienced by a lubricant in service, accounting for significant lubricant problems. It is responsible for viscosity increase, varnish formation, sludge and sediment formation, additive depletion, base oil breakdown, filter plugging, loss in foam properties, acid number increase, rust and corrosion [31]. Besides the oxygen concentration, oxidation is also influenced by other factors, such as the environment temperature and the presence of catalyst, *e.g.* water and wear metal ions.

Unlike oxidation, thermal decomposition occurs at high temperatures without oxygen. This mechanism comprises (i) micro-dieseling and (ii) electrostatic spark discharge [32]. Micro-dieseling (pressure-induced thermal degradation) occurs when an air bubble moves from a low pressure to a high pressure zone resulting in adiabatic compression and localized temperatures beyond 1000 °C. Electrostatic spark discharge can occur when clean and dry oil rapidly flows through tight clearances: internal friction in the lubricant can generate static electricity and accumulate until a sudden spark occurs at an estimated temperature of between 10,000 °C and 20,000 °C.

Water contamination in a lubricant can exist in three states. It starts when water molecules are dispersed evenly in the lubricant. When the maximum level of dissolved water in the lubricant is reached, microscopic water droplets are uniformly distributed in the lubricant: an emulsion is formed. When sufficient water is added, the two phases are separated resulting in free water in the lubricant. The two most harmful phases are the emulsified and free water phases. Effects of water in the lubricant include rust and corrosion, erosion, water etching and hydrogen embrittlement [33]. In addition, water can also: (i) accelerate oxidation, (ii) deplete oxidation inhibitors and demulsifiers, (iii) precipitate additives and (iv) compete with polar additives such as friction modifiers for metal surfaces. More explanation regarding lubricant-water interaction can be found in [34].

Excessive shear load can also be another source of lubricant degradation, where the molecular chain of viscosity modifiers breaks-down resulting in permanent viscosity loss [35,36]. A fairly detailed overview of ATF degradation mechanisms is given in [37].

1.2. Problem statement

Development of condition monitoring techniques for wet friction clutches, which are one of the critical components in automatic transmissions, has been gaining attention since the last decade. Several (destructive) methods have been proposed in the literature for clutch condition monitoring purposes, *e.g.* pressure differential scanning calorimetry (PDSC) and attenuated total internal reflectance infrared (ATR-IR) spectroscopy [38]. These two methods are not practically implementable while a clutch is under operation, owing to the fact that the friction discs have to be taken out from the clutch pack and then prepared for assessing the degradation level. Another condition monitoring method, which is non-destructive and has been used for many years, is based on tracking the mean COF (*i.e.* averaged value of the instantaneous COF for one duty cycle) of a wet friction clutch [39,30,28,40]. However, extracting the mean COF for clutch condition monitoring purpose requires *at least* two physical quantities, namely (i) the transmitted torque and (ii) the applied normal (axial) load. The applied normal load can be roughly estimated from the measured pressure (*i.e.* pressure sensors are available in some transmissions). However, the transmitted torque cannot be measured in practice because of the absence of torque sensors in real transmissions. Hence, an online condition monitoring system cannot be realized by using these existing methods.

In order to fill this substantial gap, two affordable clutch condition monitoring methods have been developed recently in the previous work [15,16] based on signals typically measured (available) in wet friction clutch applications, namely rotational velocity and pressure signals. As such, the developed monitoring methods may allow us for the practical implementation without requirement of any extra sensors. The first method is named as the *post-lockup* feature based clutch condition monitoring [16] and the second one is referred to as the *pre-lockup* feature based clutch condition monitoring method [15]. Here, the names imply how the corresponding features are extracted from different segments of the signal of interest.

The *post-lockup* features are the torsional modal parameters, namely the dominant torsional natural frequency and the corresponding damping factor. The theoretical framework of the relevance of the post-lockup features for clutch condition monitoring is discussed in [16,41], wherein the relationships between the clutch degradation level, represented by the torsional contact stiffness and damping, and the post-lockup features are straightforward. Unlike the post-lockup features, the theoretical framework of the *pre-lockup* features is not well established yet. Instead, in the previous work [15,41], the pre-lockup features were developed based on a heuristic reasoning. The relevance and robustness of the latter features have been experimentally verified with accelerated life data of some commercial wet friction clutches.

1.3. Objective

In this paper, a theoretical framework that is inspired from the underlying physical phenomenon is established for derivation of the *pre-lockup* features useful for clutch condition monitoring. It is believed that the established theoretical framework can improve our insight into the relationship between the pre-lockup features and the clutch degradation level. Furthermore, the derivation can lead to better understanding of the effect of the operational variables (*e.g.* pressure and temperature) on the features behavior that is of importance for algorithms development required for accurate health assessment and remaining useful life prediction (prognostics) of automatic transmission clutches.

1.4. Paper organization

The remainder of the paper is organized as follows. In Section 2, the *pre-lockup* based clutch condition monitoring method is briefly revisited. A theoretical framework for derivation of the pre-lockup features is established in Section 3, wherein the theoretical correlations between the pre-lockup features and the mean coefficient of friction (COF) are discussed. In addition, the latter section also discusses the sensitivity of the pre-lockup features due to any variations of the operational variables. Section 4 provides experimental verification of the developed theoretical framework. Finally, some important remarks drawn from this work are discussed in Section 5.

2. The pre-lockup feature based clutch condition monitoring method revisited

As been experimentally verified in the previous work [15], the three previously developed pre-lockup features, namely the *engagement duration* feature τ_e and *two dissimilarity* features (D_E and D_{SAM}), are strongly correlated. The engagement duration feature constitutes a physical quantity, while the other two features are non-physical features which are widely applied in machine learning community. For clutch condition monitoring purpose, one can either use one of the three features only or combine them by means of the logistic regression as discussed in another work [42].

Fig. 5 shows the flowchart of the signal processing and the feature extraction developed for the pre-lockup feature based clutch condition monitoring method. It is seen in the figure that three (typically available) signals, *i.e.* the *input* rotational velocity signal ω_i, the *output* rotational velocity signal ω_o and the pressure signal p, are required. In practice, these three signals are digital (discrete-time) signals with the same time record length. For convenience, the digital version of these signals is respectively written as $\omega_{i,k}$, $\omega_{o,k}$ and p_k, with $k = 1, 2, \ldots, M$.

As the first step, the *reference time instant* t_f is determined from the digital pressure signal p_k, namely by linearly interpolating the two consecutive discrete-time instants t_K and t_{K+1}, for which the index $K < M$ is computed according to the following equation:

$$K = \min\{\forall k \in \mathbb{Z} : (p_k - p_{lim}) * (p_{k+1} - p_{lim}) < 0\}, \tag{1}$$

where $p_{lim} > 0$ denotes the pressure threshold that needs to be pre-determined by the user and $\mathbb{Z}$ denotes the set of positive integers. Note that Eq. (1) summarizes the well-known simple algorithm that searches the first index of a-certain-level-crossing in a discrete-time signal.

In parallel to the first step, the (discrete-time) raw relative rotational velocity signal $\omega_{r,k}$, with $k = 1, 2, \ldots, M$, is also calculated by *vector subtraction* of $\omega_{i,k}$ with $\omega_{o,k}$. Then, as the key step, the relative rotational velocity signal of interest, hereafter called the *signal of interest* $\omega_{r,l|soi}$; with $l = 1, 2, \ldots, N$, is captured from $\omega_{r,k}$ by the *SOI recorder*. It should be addressed here that the captured signal of interest $\omega_{r,l|soi}$ is a truncated version of the raw signal $\omega_{r,k}$ so that the time record length of $\omega_{r,l|soi}$ is shorter than the record length of $\omega_{r,k}$, *i.e.* $N = M - K$. The signal of interest $\omega_{r,l|soi}$ is mathematically defined as

$$\omega_{r,l|soi} = \omega_{r,K<k\le M}. \tag{2}$$

Subsequently, the *lockup time instant* t_l is predicted from $\omega_{r,l|soi}$, by linearly interpolating the two consecutive discrete-time instants t_L and t_{L+1}, for which the index $L < N$ is calculated based on the following equation:

$$L = \min\{\forall l \in \mathbb{Z} : (\omega_{r,l|soi} - \omega_{r,lim|soi}) * (\omega_{r,l+1|soi} - \omega_{r,lim|soi}) < 0\}, \tag{3}$$

where $\omega_{r,lim|soi} > 0$ denotes the pre-determined threshold of the digital signal of interest $\omega_{r,l|soi}$. Note here that Eq. (3) is similar to Eq. (1), *i.e.* simply searching the first time index of a-value-crossing in a discrete-time signal.

For convenience, the reference time instant t_f of $\omega_{r,l|soi}$ can be set to zero (*i.e.* $t_f = 0$), so the engagement duration feature τ_e can now be simply calculated as follows:

$$\tau_e = t_l - t_f = t_l. \tag{4}$$

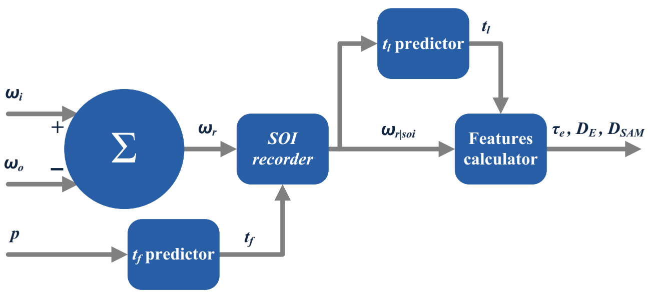

Fig. 5. Procedure of the signal processing and feature extraction.

3. Theoretical development

3.1. Derivation of the pre-lockup features

Since the clutch degradation level can be represented by the mean COF, *i.e.* averaged value of the instantaneous COFs of a given duty cycle, [39,30,28,40], it is therefore important to search for measurable parameters that are correlated to the mean COF. For this purpose, let us consider the clutch engagement process (*i.e.* pre-lockup phase) illustrated in Fig. 3. In this phase, both input and output inertias are decoupled so that the clutch system can be simply modeled as two inertias moving independently. Since rotational motion (which is the nature of a clutch system) has a strong analogy with translational motion, for the sake of simplicity, the clutch system is therefore analyzed on the translational equivalent as illustrated in Fig. 6.

As shown in the figure, the input and output inertias of a wet clutch system are represented by the two rigid bodies m_1 and m_2. Note that this illustration is seen from the top view and the two bodies are lying on a frictionless surface. To represent the filling phase (ii), the two bodies are independently moving with the corresponding initial velocities of $v_{0,1}$ and $v_{0,2}$ and respectively driven by the forces of F_1 and F_2. Without loss of generality, let us assume that $v_{0,1} > v_{0,2}$ and the driving forces are constant. A lateral force F_N is applied on the side of each body such that the two masses are brought into contact. Here, the velocities of the two bodies when brought into *contact for the first time* at the time instant t_i are the same as the initial velocities $v_{0,1}$ and $v_{0,2}$. Because of the relative motion between the bodies, a friction force occurs on the contacting surface with the mean COF of μ. Finally, the two bodies move together with the same velocity v_l, which equivalently corresponds to the post-lockup phase.

With the aid of the basic physics, analysis on the system in Fig. 6 leads to the fact that the engagement duration τ_e and the sliding distance s, which are measurable, are correlated to the mean COF μ. These correlations are expressed in Eqs. (5) and (6) and the proof can be found in Appendix A.

$$\tau_e = \frac{m_{eq} v_0}{\mu F_N - F_{eq}} \tag{5}$$

$$s = \frac{m_{eq} v_0^2}{2(\mu F_N - F_{eq})}, \tag{6}$$

with

$$\begin{aligned} v_0 &= v_{0,1} - v_{0,2}, \\ m_{eq} &= \frac{m_1 m_2}{m_1 + m_2}, \\ \alpha &= \frac{m_1}{m_1 + m_2}, \\ F_{eq} &= (1-\alpha)F_1 - \alpha F_2 < \mu F_N. \end{aligned}$$

3.2. Analysis of the features

The previous section has theoretically revealed that the engagement duration τ_e and the sliding distance s are *inversely proportional* to the mean COF μ. However, these relationships need to be experimentally verified as will be discussed in Section 4. To this end, Pearson's correlation coefficient ρ is considered in this study as a metric to qualify the relationships. This metric will be shortly discussed in the following subsection.

Besides the correlation, the sensitivity of the two features (engagement duration and the sliding distance) due to changes of their variables needs to be investigated as well. Such an investigation is important to clearly distinguish between the effects of the operational variables (namely the initial sliding velocity v_0 and normal load F_N) and the degradation variable

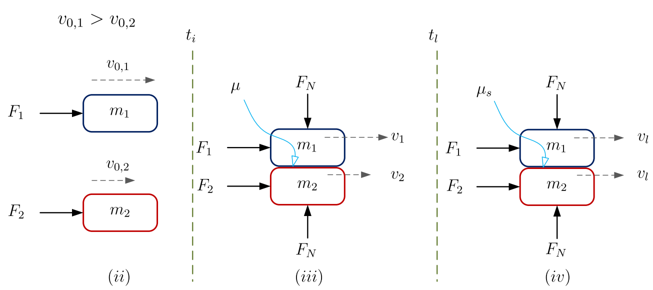

Fig. 6. The translational equivalent of a wet friction clutch system (top view).

(namely the mean COF μ) on the behavior of both features. This understanding can aid in developing a strategy for realizing an accurate clutch monitoring system.

Remark 1. Unlike the engagement duration feature τ_e, the computation of the sliding distance feature s from measurement signals (*i.e.* discrete data) has not been discussed yet in the previous sections. Assume that the (discrete) signal of interest $\omega_{r,l|soi}$, $l=1,2,\ldots,N$, obtained from the procedure described in Fig. 5, is given. Hence, the sliding distance s can be computed from the signal of interest by the following equation:

$$s=\tau_s\sum_{l=1}^{L}\omega_{r,l|soi}, \tag{7}$$

where τ_s denotes the sampling period and $L<N$ is determined based on Eq. (3).

3.2.1. Correlation analysis: Pearson's correlation coefficient

Assume that two discrete quantities, x_i and y_i, $i=1,2,\ldots,N$, are obtained from a set of experiments. Pearson's correlation coefficient ρ of the two quantities is mathematically defined as [43]

$$\rho=\frac{\sum_{i=1}^{N}(x_i-\overline{x})(y_i-\overline{y})}{\sqrt{\sum_{i=1}^{N}(x_i-\overline{x})^2}\sqrt{\sum_{i=1}^{N}(y_i-\overline{y})^2}}, \tag{8}$$

with

$$\overline{x}=\frac{1}{N}\sum_{i=1}^{N}x_i, \tag{9}$$

$$\overline{y}=\frac{1}{N}\sum_{i=1}^{N}y_i. \tag{10}$$

Eq. (8) implies that the values of the correlation coefficient lie between -1 and $+1$. When the values of the coefficient are close to -1, it is known that the dependency between two variables is *inversely* proportional. On the other hand, the dependency is *linearly* proportional when the values are close to $+1$.

3.2.2. Sensitivity analysis

Let us reevaluate the expressions of the engagement duration τ_e and sliding distance s given in Eqs. (5) and (6) respectively. The total derivatives of τ_e and s in function of all relevant variables μ, F_N, v_0 and F_{eq} can be formulated as follows:

$$d\tau_e=\frac{\partial\tau_e}{\partial\mu}d\mu+\frac{\partial\tau_e}{\partial F_N}dF_N+\frac{\partial\tau_e}{\partial v_0}dv_0+\frac{\partial\tau_e}{\partial F_{eq}}dF_{eq}, \tag{11}$$

and

$$ds=\frac{\partial s}{\partial\mu}d\mu+\frac{\partial s}{\partial F_N}dF_N+\frac{\partial s}{\partial v_0}dv_0+\frac{\partial s}{\partial F_{eq}}dF_{eq}. \tag{12}$$

By solving the latter equations with the help of Eqs. (5) and (6), one can show that the total derivatives of τ_e and s can be expressed as follows:

$$d\tau_e=\tau_e\left[-\frac{d\mu}{\mu(1-\beta)}-\frac{dF_N}{F_N(1-\beta)}+\frac{dv_0}{v_0}+\frac{dF_{eq}}{F_{eq}(1/\beta-1)}\right], \tag{13}$$

and

$$ds=s\left[-\frac{d\mu}{\mu(1-\beta)}-\frac{dF_N}{F_N(1-\beta)}+\frac{2dv_0}{v_0}+\frac{dF_{eq}}{F_{eq}(1/\beta-1)}\right], \tag{14}$$

with

$$0<\beta=\frac{F_{eq}}{\mu F_N}<1.$$

For large changes, Eqs. (13) and (14) can be rewritten as follows:

$$\frac{\Delta\tau_e}{\tau_e}=-\frac{\Delta\mu}{\mu(1-\beta)}-\frac{\Delta F_N}{F_N(1-\beta)}+\frac{\Delta v_0}{v_0}+\frac{\Delta F_{eq}}{F_{eq}(1/\beta-1)}, \tag{15}$$

and

$$\frac{\Delta s}{s}=-\frac{\Delta\mu}{\mu(1-\beta)}-\frac{\Delta F_N}{F_N(1-\beta)}+\frac{2\Delta v_0}{v_0}+\frac{\Delta F_{eq}}{F_{eq}(1/\beta-1)}. \tag{16}$$

It is clear now from Eqs. (15) and (16) that variations of the two features ($\Delta\tau_e$ and Δs) have a *negative* correlation with variations of the mean COF $\Delta\mu$ and the normal force ΔF_N. On the other hand, variations of the two features have a *positive* correlation with a variation of the initial relative velocity Δv_0 and the external force ΔF_{eq}. Surprisingly, a variation of the initial sliding velocity Δv_0 gives a *two times larger* on the variation of the sliding distance Δs compared to that of the engagement time $\Delta\tau_e$.

For clutch condition monitoring purposes, where the change of degradation level (state) that is represented by the mean COF μ is tracked based on feature is of interest, the variations of the operational variables, namely pressure variation Δp (equivalent to ΔF_N), variation of the initial relative rotational velocity $\Delta\omega_{trig}$ (equivalent to Δv_0) and variation of the input and output torque $\Delta M_i, \Delta M_o$ (equivalent to ΔF_{eq}), should be minimized in order to achieve an accurate assessment of the clutch condition. One possible strategy to realize this is by embedding the aforementioned control routine in the ECU, where the control signal sent to the control valve for a clutch actuation is triggered if the pre-defined initial relative velocity ω_{trig} is detected. In terms of minimizing the variation of the applied normal force (pressure) Δp, the control signal sent to the valve should be kept the same.

Depending on the type of the used oil/automatic transmission fluid (ATF), a variation of the oil temperature ΔT can have a significant contribution to the variation of the mean COF $\Delta\mu$. Thus, when monitoring the condition of a wet clutch using the proposed features is of interest, the oil temperature variation should be minimized in order to achieve an accurate assessment. In practice, controlling the oil temperature of a wet clutch to a certain value is a difficult task. However, minimizing the oil temperature variation for clutch condition monitoring purpose is still feasible by embedding an acquisition routine in the ECU, where all the relevant signals are *only recorded and processed* when the oil temperature lies in a certain temperature range. This suggests that the use of a temperature sensor has an added value for realizing an accurate condition monitoring system based on the proposed method.

Ideally, if variations of all the operational variables ($\Delta\omega_{trig}$, Δp, ΔM_i, ΔM_o and ΔT) are negligible, the relationships between the two features and the mean COF become simple:

$$\frac{\Delta s}{s} = \frac{\Delta\tau_e}{\tau_e} = -\frac{\Delta\mu}{\mu(1-\beta)}, \tag{17}$$

4. Experimental verification and discussions

To experimentally verify the theory developed in the previous section, the first four datasets used in the previous investigations [15,16] are reanalyzed in this paper. Notice that the data are obtained from accelerated life tests (ALTs) carried out on different *commercial* wet friction clutches using a fully instrumented SAE#2 test setup under the *same* operating conditions (laboratory environment). All the tests were carried out until 10,000 duty cycles with relatively high energy dissipation. For further description of the experiments, interested readers are referred to [15,16].

During the tests, the initial input and output rotational velocities, i.e. $\omega_{i,trig}$ and $\omega_{o,trig}$, applied pressure p and inlet oil temperature T_{inlet} were controlled at approximately the same corresponding values for each clutch duty cycle. In addition, no torques were applied on the input and output flywheels, i.e. $M_o = M_i = 0$. In this way, the contribution of any variations of the operational variables to the variations of the two features is expected to be negligible. Hence, any variations of the two features are mainly due to the degradation occurring in the clutches. Fig. 7 shows the histograms of the *mean values* of the operational variables for different duty cycles. As can be seen in Table 1, the variations in percentage of the operational variables are in general less than 5%.

4.1. Verification of the features behavior

By applying the feature extraction procedure described earlier, the two features can be computed from the signal of interest. It is important to note here that the signals of interest for different duty cycles and ALTs can be found in [15]. Additionally, the procedure to compute the mean COF from relevant signals for every duty cycle is also discussed therein.

Fig. 8 shows the evolution of the features and the mean COF in a function of the duty cycles obtained from different ALTs. It is seen from the figure that as the degradation progresses the mean COFs drop which confirm experimental evidence reported in the literature, for example see Refs. [30,40]. Furthermore, one can clearly see that the trend of the mean COF is opposite from the trends of the two features. Hence, this experimental evidence confirms that the theoretical predictions discussed in Section 3 are verified.

Remarkably, the trends of the features show a (*quasi*) linear behavior with relatively small variations. These small variations are theoretically plausible since the variations of the operational variables are relatively small (*i.e.* less than 5%) as shown in Table 1. Hence, as expected, the trends are mainly due to the clutch degradation. For comparison purposes, the features (τ_e and s) and the mean COF μ are normalized according to the following equations:

$$\hat{\mu} = \frac{\mu - \mu^{ref}}{\mu^{ref}} \tag{18}$$

$$\hat{\tau_e} = \frac{\tau_e - \tau_e^{ref}}{\tau_e^{ref}} \tag{19}$$

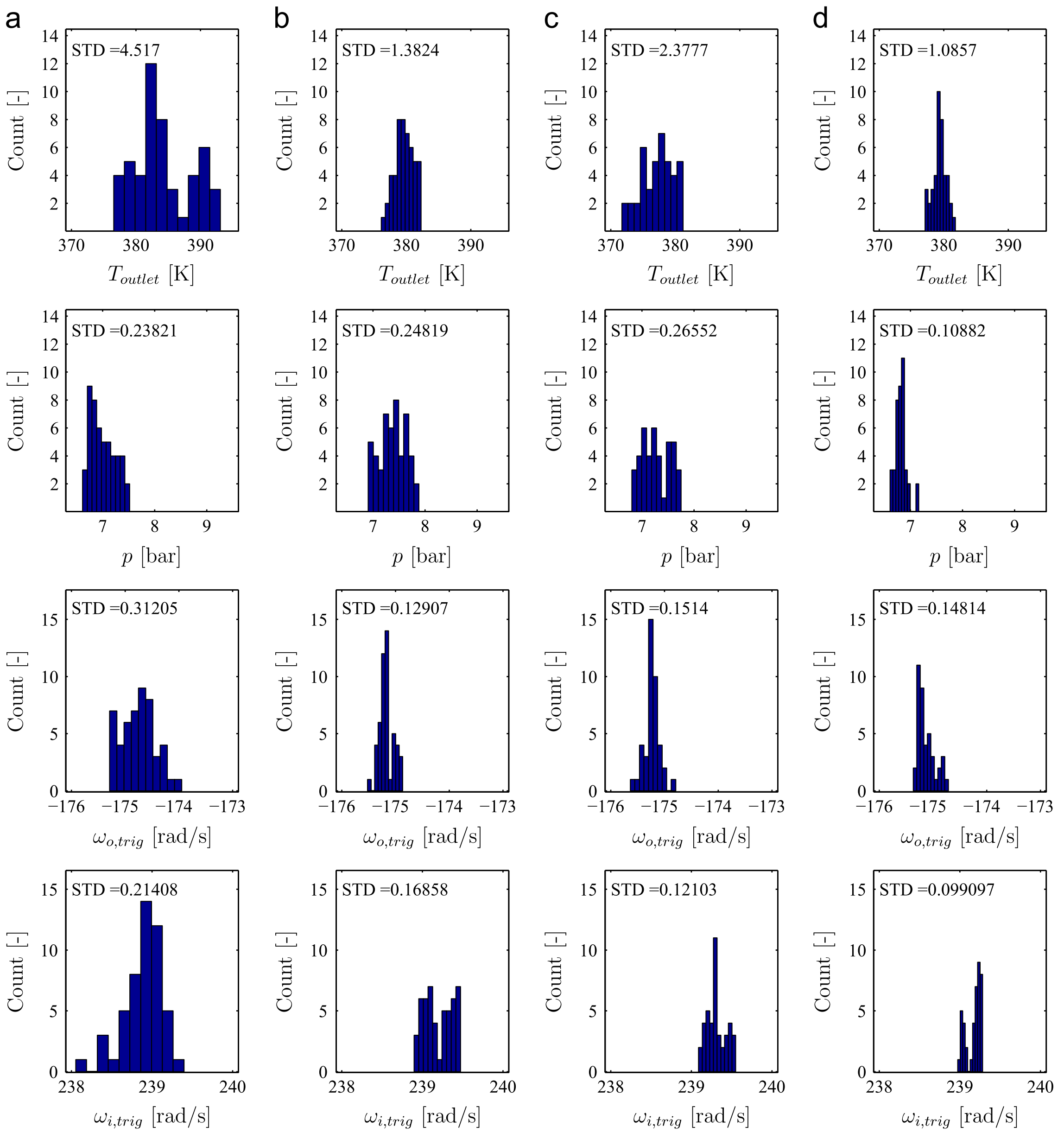

Fig. 7. Histograms of the *mean values* of the operational variables for different duty cycles. (a) 1st ALT, (b) 2nd ALT, (c) 3rd ALT and (d) 4th ALT. Note that the negative sign of $\omega_{o,trig}$ indicates opposite direction with respect to $\omega_{i,trig}$.

Table 1
Variations in percentage of the *mean values* of the operational variables for different duty cycles.

#ALT	$100 \times \left\lvert \frac{\Delta\omega_{i,trig}}{\omega_{trig}} \right\rvert$	$100 \times \left\lvert \frac{\Delta\omega_{o,trig}}{\omega_{trig}} \right\rvert$	$100 \times \left\lvert \frac{\Delta p}{p} \right\rvert$	$100 \times \left\lvert \frac{\Delta T_{outlet}}{T_{outlet}} \right\rvert$
1	0.09	0.18	3.46	1.20
2	0.07	0.07	3.44	0.36
3	0.05	0.09	3.60	0.63
4	0.04	0.08	2.25	0.29

$$\hat{s} = \frac{s - s^{ref}}{s^{ref}} \tag{20}$$

where $\hat{\mu}$, $\hat{\tau_e}$ and $\hat{s}$ respectively denote the normalized mean COF, normalized engagement duration and normalized sliding distance, with $[\cdot]^{ref}$ denoting the reference values obtained at an initial duty cycle.

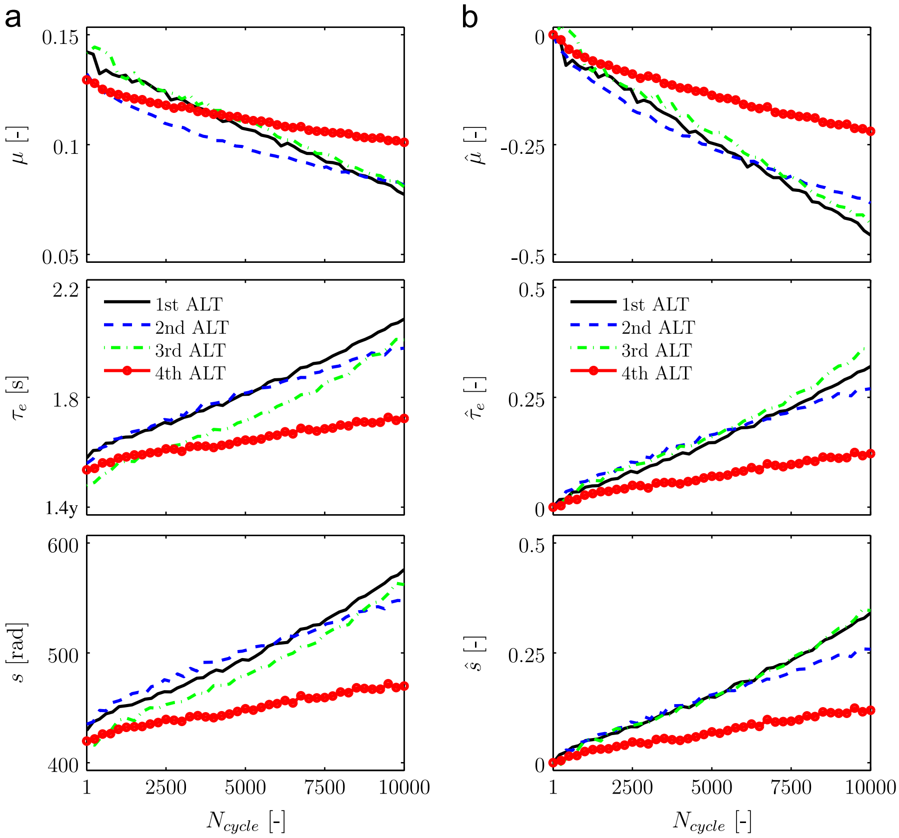

Fig. 8. Comparison of the evolution of the mean COF μ and the two features (engagement duration τ_e and sliding distance s) for different duty cycles. (a) Absolute values and (b) normalized values.

Fig. 8(b) shows the evolution of the normalized features and the mean COF. As can be seen in the figure, the *absolute* changes of the two normalized features ($\hat{\tau_e}$ and $\hat{s}$) after 10,000 duty cycles are the same for the four ALTs as theoretically predicted, but the absolute changes of the normalized mean COF $\hat{\mu}$ are larger than those of the two normalized features. Nevertheless, the absolute changes of the three normalized quantities after 10,000 duty cycles are in the same order of magnitude, thus reasonably confirming Eq. (17).

4.2. Correlation analysis

In order to verify the theoretical relationships between the features and the mean COF discussed previously, the correlation coefficients of $\hat{\tau_e}$ vs. $\hat{\mu}$ and $\hat{s}$ vs. $\hat{\mu}$ according to Eq. (8) have been computed for different ALTs. Fig. 9 shows the experimental correlations of the two normalized features with the normalized mean COF. Visually, it is obvious from the figure that the relationships are inversely proportional. The relationships are verified by the correlation coefficient values, which are very close to -1, as listed in Table 2.

5. Concluding remarks

The theoretical derivation of the *pre-lockup* features useful for wet friction clutch condition monitoring is discussed in this paper. It is shown theoretically that the two pre-lockup features are *inversely proportional* to the mean coefficient of friction (COF). To verify the theoretical predictions, Pearson′s correlation coefficients have been computed on the experimental data obtained from accelerated life tests of some commercial wet friction clutches using a fully instrumented SAE#2 test setup. The values of the coefficient are very close to -1, thus verifying the theoretical predictions.

In order to achieve an accurate condition monitoring method, it is theoretically revealed that the variations of some operational variables, namely (i) the oil temperature, (ii) actuation pressure and (iii) initial relative rotational velocity, should be kept as small as possible. For practical implementation, this can be realized by embedding some control and acquisition related-routines into the Engineering Control Unit (ECU) that can satisfy the aforementioned requirements. The nature of the proposed signal processing and feature extraction implies that the *pre-lockup* features are suitable for condition monitoring of wet friction clutches used in both traditional automatic transmissions (ATs) and dual clutch

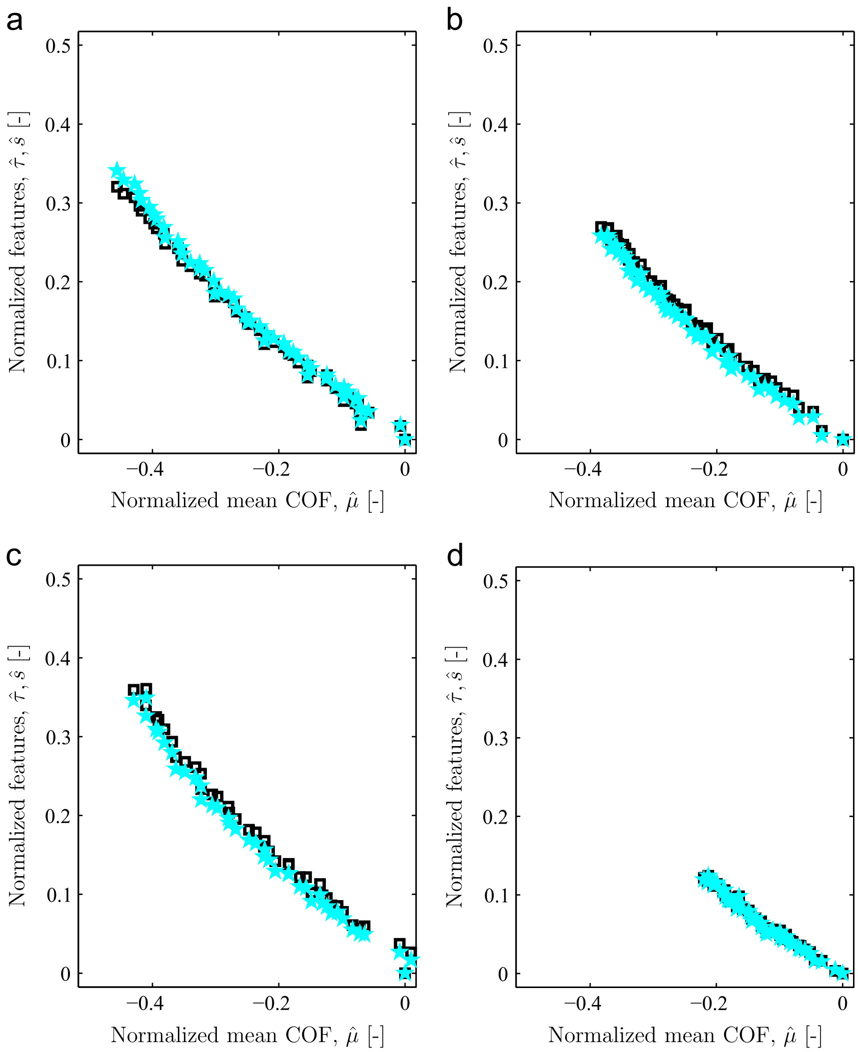

Fig. 9. Experimental relationship of the two features (*i.e.* τ_e and s) vs. the mean COF μ obtained from (a) ALT#1, (b) ALT#2, (c) ALT#3 and (d) ALT#4. Note that the marker □denotes ρ_1: $\hat{\tau_e}$ vs. $\hat{\mu}$ and the marker $\star$ denotes ρ_2: $\hat{s}$ vs. $\hat{\mu}$.

Table 2
Correlation coefficients of $\hat{\tau_e}$ vs. $\hat{\mu}$ and $\hat{s}$ vs. $\hat{\mu}$ for different ALTs.

#ALT	$\rho_1 : \hat{\tau_e}$ vs. $\hat{\mu}$	$\rho_2 : \hat{s}$ vs. $\hat{\mu}$
1	−0.994	−0.992
2	−0.994	−0.993
3	−0.989	−0.989
4	−0.992	−0.989

transmissions (DCTs), where the *initial* relative rotational velocity can be imposed at (more or less) *the same value* for different engagement cycles.

Acknowledgments

The author wishes to thank Dr. Mark Versteyhe of Dana Spicer Off Highway Belgium for sharing the experimental data. The author also gratefully acknowledges the two anonymous reviewers for their constructive comments on the manuscript. The scientific responsibility is assumed by its author.

Appendix A

The formal relationships of the engagement duration versus the mean COF (τ_e vs. μ) and the sliding distance versus the mean COF (s vs. μ) expressed in Eqs. (5) and (6) can be summarized in Theorem 1.

Theorem 1. *Let μ be denoting the mean COF of a clutch for a certain engagement cycle, and let τ_e and s be denoting the engagement duration and the sliding distance, respectively. Suppose that these three parameters are positive values. Then $\tau_e \propto 1/\mu$ and $s \propto 1/\mu$.*

Proof. The equations of motion of the two bodies m_1, m_2 in Fig. 6, assuming $v_{0,1} > v_{0,2}$, can be expressed as follows:

$$F_1 - f = m_1 \frac{dv_1}{dt}, \tag{A.1}$$

$$F_2 + f = m_2 \frac{dv_2}{dt}, \tag{A.2}$$

with $f = \mu F_N$. By calculating the impulse of the driving force and the momentum of each body from the time instant t_i to a given time instant t, the instantaneous velocity of each body (v_1, v_2) can then be determined, i.e.:

$$\int_{t_i}^{t} (F_1 - \mu F_N)\, dt = \int_{v_{0,1}}^{v_1} m_1\, dv_1, \tag{A.3}$$

$$v_1 = v_{0,1} + \frac{(F_1 - \mu F_N)(t - t_i)}{m_1}, \tag{A.4}$$

$$\int_{t_i}^{t} (F_2 + \mu F_N)\, dt = \int_{v_{0,2}}^{v_2} m_2\, dv_2, \tag{A.5}$$

$$v_2 = v_{0,2} + \frac{(F_2 + \mu F_N)(t - t_i)}{m_2}. \tag{A.6}$$

For the sake of simplicity, the time instant t_i can be set to zero, so the velocities of the two bodies at given time instant t can be rewritten as follows:

$$v_1 = v_{0,1} + \frac{(F_1 - \mu F_N)t}{m_1}, \tag{A.7}$$

$$v_2 = v_{0,2} + \frac{(F_2 + \mu F_N)t}{m_2}. \tag{A.8}$$

At the lockup time instant t_l, the two bodies have the same velocity, i.e. $v_1 = v_2 = v_l$. The time interval from t_i to t_l, which is referred to as the engagement duration $\tau_e = t_l - t_i$, can be determined by equating Eq. (A.7) with Eq. (A.8). One can easily show that the engagement duration τ_e can be expressed according to the following equation:

$$\tau_e = \frac{m_{eq} v_0}{\mu F_N - F_{eq}}, \tag{A.9}$$

with

$$v_0 = v_{0,1} - v_{0,2},$$
$$m_{eq} = \frac{m_1 m_2}{m_1 + m_2},$$
$$\alpha = \frac{m_1}{m_1 + m_2},$$
$$F_{eq} = (1-\alpha)F_1 - \alpha F_2.$$

Let v_r be defined as the instantaneous relative velocity between the two bodies, i.e.

$$v_r = v_1 - v_2. \tag{A.10}$$

Furthermore, substituting Eqs. (A.7) and (A.8) into Eq. (A.10), the relative velocity v_r can then be expressed as

$$v_r = v_0 + \left(\frac{F_1}{m_1} - \frac{F_2}{m_2}\right)t - \frac{\mu F_N}{m_e q} t. \tag{A.11}$$

Let us now define the sliding distance s as the total relative displacement between the two bodies from the time instant t_i to t_l. Mathematically, the sliding distance s can be calculated by integrating the relative velocity v_r over the time interval, i.e.

$$s = \int_{t_i}^{t_l} v_r\, dt = \int_0^{\tau_e} v_r\, dt. \tag{A.12}$$

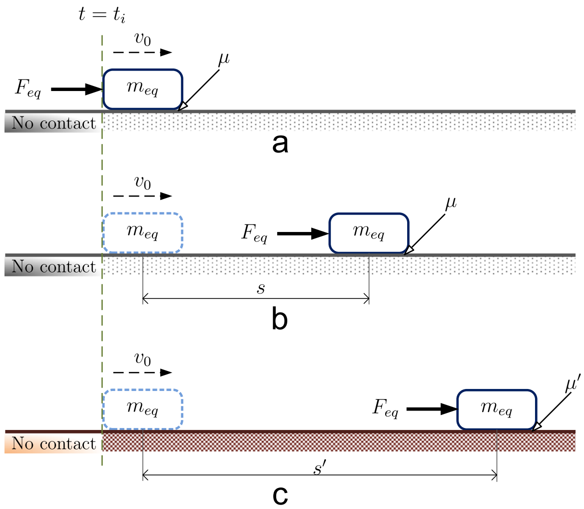

Fig. B1. A scheme illustrating the relationship between the coefficient of friction (COF) μ and the sliding distance s of a simple tribological system. Note that $\mu' < \mu$.

Solving Eq. (A.12) with the aid of Eqs. (A.9) and (A.11), one can show that the sliding distance s is expressible as follows:

$$s = \frac{m_{eq} v_0^2}{2(\mu F_N - F_{eq})}, \tag{A.13}$$

Appendix B

To further illustrate the correlations of the mean COF vs. the engagement duration and the mean COF vs. the sliding distance, the system of the two rigid bodies shown in Fig. 6 can be *reduced* into a single rigid body of equivalent mass m_{eq} subjected to a constant driving force F_{eq} lying on a surface as illustrated in Fig. B1(a). Assume without loss of generality that the contact between the body and the surface is established after the time instant t_i and the *mean* COF μ between the body and the surface, at a given degradation level (say a healthy state), is constant. Moreover, let us assume that the body is subjected to a constant normal load, *i.e.* its own weight. Due to the friction, the rigid body will stop after having displacement of s with respect to its initial position as schematically illustrated in Fig. B1(b).

Let us now consider another case wherein the rigid body is placed on another surface representing a degraded state of a wet friction clutch, where the mean COF is lower than that in the healthy state ($\mu' < \mu$). It should be noticed that this particular case is relevant since the mean COF of a wet friction clutch typically decreases due to the progression of both material and oil degradation [40,44]. One can immediately deduce that the sliding distance in the latter state will be larger than that of the healthy state, *i.e.* $\mu' < \mu \rightarrow s' > s$, compare Fig. B1(b) and (c). Equivalently, the engagement duration in the degraded state will be longer than the one in the healthy state, *i.e.* $\mu' < \mu \rightarrow \tau_e' > \tau_e$.

References

[1] M. Versteyhe, IWT proposal (in Dutch), Technical Report, Dana-Spicer Off Highway, Belgium, 2011.
[2] A.P. Ompusunggu, Intelligent monitoring and prognostics of automotive clutches (Ph.D. thesis), Katholieke Universiteit Leuven, Department of Mechanical Engineering, Division PMA, Belgium, 2012.
[3] T. Kugiyama, N. Yoshimura, J. Mitsui, Tribology of automatic transmission fluid, Tribol. Lett. 5 (1998) 49–56.
[4] A. Haj-Fraj, F. Pfeiffer, Dynamic modeling and analysis of automatic transmissions, in: Proceedings of IEEE/ASME International Conference on Advanced Intelligent Mechatronics, 1999, pp. 1026–1031.
[5] A. Crowther, N. Zhang, D.K. Liu, J.K. Jeyakumaran, Analysis and simulation of clutch engagement judder and stick-slip in automotive powertrain systems, Proc. Inst. Mech. Eng. Part D: J. Autom. Eng. 218 (12) (2004) 1427–1446. arXiv:http://pid.sagepub.com/content/218/12/1427.full.pdf+html.
[6] J. Kim, Launching performance analysis of a continuously variable transmission vehicle with different torsional couplings, J. Mech. Des. 127 (2) (2005) 295–301.
[7] J. Deur, J. Asgari, D. Hrovat, Modeling and analysis of automatic transmission engagement dynamics-nonlinear case including validation, J. Dyn. Syst. Meas. Control 128 (2) (2006) 251–262.
[8] Z. Sun, K. Hebbale, Challenges and opportunities in automotive transmission control, in: Proceedings of 2005 American Control Conference, vol. 5, 2005, pp. 3284–3289.
[9] L. Glielmo, L. Iannelli, V. Vacca, F. Vasca, Gearshift control for automated manual transmissions, IEEE/ASME Trans. Mechatron. 11 (1) (2006) 17–26.
[10] D. Kim, H. Peng, S. Bai, J.M. Maguire, Control of integrated powertrain with electronic throttle and automatic transmission, IEEE Trans. Control Syst. Technol. 15 (3) (2007) 474–482.
[11] T. Janssens, Dynamic characterisation and modelling of dry and boundary lubricated friction for stabilisation and control purposes (Ph.D. thesis), Katholieke Unversiteit Leuven, Department of Mechanical Engineering, Division PMA, Belgium, February, 2010.

[12] B.Z. Gao, H. Chen, K. Sanada, Y. Hu, Design of clutch-slip controller for automatic transmission using backstepping, IEEE/ASME Trans. Mechatron. 16 (3) (2011) 498–508.
[13] M. Zhou, S. Zhang, J. Wen, X. Wang, Research on CVT fault diagnosis system based on artificial neural network, in: Vehicle Power and Propulsion Conference, 2008, VPPC ′08, IEEE, 2008, pp. 1–5.
[14] H. Kong, G. Ren, J. He, B. Xiao, The application of fuzzy neural network in fault self-diagnosis system of automatic transmission, J. Softw. 6 (2) (2011) 209–216. http://dx.doi.org/10.4304/jsw.6.2.209-216.
[15] A.P. Ompusunggu, J.-M. Papy, S. Vandenplas, P. Sas, H. VanBrussel, Condition monitoring method for automatic transmission clutches, Int. J. Progn. Health Manag. (IJPHM) Soc. 3 (2012) 19–32.
[16] A.P. Ompusunggu, J.-M. Papy, S. Vandenplas, P. Sas, H. VanBrussel, A novel monitoring method of wet friction clutches based on the post-lockup torsional vibration signal, Mech. Syst. Signal Process. 35 (2013) 345–368.
[17] R.K. Mobley, An Introduction to Predictive Maintenance, Butterworth-Heinemann, 2002.
[18] M. Basseville, A. Benveniste, B. Gach-Devauchelle, M. Goursat, D. Bonnecase, P. Dorey, M. Prevosto, M. Olagnon, In situ damage monitoring in vibration mechanics: diagnostics and predictive maintenance, Mech. Syst. Signal Process. 7 (5) (1993) 401–423.
[19] D. Bansal, D.J. Evans, B. Jones, A real-time predictive maintenance system for machine systems, Int. J. Mach. Tools Manuf. 44 (7–8) (2004) 759–766.
[20] M.C. Garcia, M.A. Sanz-Bobi, J. del Pico, SIMAP: Intelligent system for predictive maintenance: application to the health condition monitoring of a wind turbine gearbox, Comput. Ind. 57 (6) (2006) 552–568.
[21] J. Srinivas, B.S.N. Murthy, S.H. Yang, Damage diagnosis in drive-lines using response-based optimization, Proc. Inst. Mech. Eng. Part D: J. Autom. Eng. 221 (11) (2007) 1399–1404.
[22] A. Bey-Temsamani, M. Engels, A. Motten, S. Vandenplas, A.P. Ompusunggu, A practical approach to combine data mining and prognostics for improved predictive maintenance, in: The 15th ACM SIGKDD Conference on Knowledge Discovery and Data Mining, 2009.
[23] A. Bey-Temsamani, M. Engels, A. Motten, S. Vandenplas, A.P. Ompusunggu, Condition-based maintenance for OEM′s by application of data mining and prediction techniques, in: Proceedings of the 4th World Congress on Engineering Asset Management, 2009.
[24] Y. Kato, T. Shibayama, Mechanism of automatic transmissions and their requirements for wet clutches and wet brakes, Jpn. J. Tribol. 39 (1994) 1427–1437.
[25] R. Mäki, Wet clutch tribology—friction characteristics in limited slip differentials (Ph.D. thesis), Luleå University of Technology, Division of Machine Elements, Sweden, 2005.
[26] N. Sakai, F. Honda, K. Nakijima, Friction characteristics of wet paper clutch for automotive torque transmissions, Lubr. Eng. 49 (2) (1993) 97–101.
[27] H. Gao, G.C. Barber, H. Chu, Friction characteristics of a paper-based friction material, Int. J. Autom. Technol. 3 (4) (2002) 171–176.
[28] S. Li, M. Devlin, S.H. Tersigni, T.C. Jao, K. Yatsunami, T.M. Cameron, Fundamentals of anti-shudder durability: Part I clutch plate study, SAE Technical Paper 2003-01-1983, 2003, pp. 51–62.
[29] T. Newcomb, M. Sparrow, B. Ciupak, Glaze analysis of friction plates, SAE Technical Paper 2006-01-3244.
[30] M. Maeda, Y. Murakami, Testing method and effect of ATF performance on degradation of wet friction materials, SAE Technical Paper 2003-01-1982, 2003, pp. 45–50.
[31] D. Wooton, The lubricant′s nemesis—oxidation, in: Practicing Oil Analysis Magazine, 2007.
[32] G. Livingstone, D. Wooton, B. Thompson, Finding the root causes of oil degradation, in: Practicing Oil Analysis Magazine, 2007.
[33] M. Duncanson, Detecting and controlling water in oil, in: Practicing Oil Analysis Magazine, 2005.
[34] M.F. Smiechowski, V.F. Lvovich, Electrochemical monitoring of water surfactant interactions in industrial lubricants, J. Electroanal. Chem. 534 (2) (2002) 171–180.
[35] B. Wright, J.P.R. du Parquet, Degradation of polymers in multigrade lubricants by mechanical shear, Polym. Degrad. Stab. 5 (1983) 425–447.
[36] I.I. Kudish, R.G. Airapetyan, Lubricants with non-newtonian rheology and their degradation in line contacts, J. Tribol. 126 (1) (2004) 112–124.
[37] K. Berglund, Sustainable performance of wet clutch systems (Master′s thesis), Luleå University of Technology, Department of Applied Physics and Mechanical Engineering, Division of Machine Elements, 2010.
[38] J.J. Guan, P.A. Willermet, R.O. Carter, D.J. Melotik, Interaction between ATFs and friction material for modulated torque converter clutches, SAE Technical Paper 981098, 1998, pp. 245–252.
[39] K. Matsuo, S. Saeki, Study on the change of friction characteristics with use in the wet clutch of automatic transmission, SAE Technical Paper 972928, 1997, pp. 93–98.
[40] J. Fei, H.-J. Li, L.-H. Qi, Y.-W. Fu, X.-T. Li, Carbon-fiber reinforced paper-based friction material: study on friction stability as a function of operating variables, J. Tribol. 130 (4) (2008) 041605.
[41] A.P. Ompusunggu, P. Sas, H. VanBrussel, Modeling and simulation of the engagement dynamics of a wet friction clutch system subjected to degradation: an application to condition monitoring and prognostics, Mechatronics 23 (6) (2013) 700–712.
[42] A.P. Ompusunggu, S. Vandenplas, P. Sas, H. VanBrussel, Health assessment and prognostics of automotive clutches, in: First European Conference of the Prognostics and Health Management Society, PHM Society, 2012.
[43] J.L. Rodgers, W.A. Nicewander, Thirteen ways to look at the correlation coefficient, Am. Stat. 42 (1) (1988) 59–66.
[44] A.P. Ompusunggu, T. Jannsens, P. Sas, Friction behavior of a wet clutch subjected to accelerated degradation, ISRN Tribol. 2013 (2013). ID 607279, 11 pages. http://dx.doi.org/10.5402/2013/607279.